Iranian Journal of Science and Technology, Transactions of Civil Engineering (2022) 46:2289–2300
https://doi.org/10.1007/s40996-022-00819-8

RESEARCH PAPER

# Assessment of New Vector Intensity Measures for the Seismic Evaluation of Low-rise Frames by Considering Near-field Aftershock Effects

**Fatemeh Soleiman Meigooni[1] · Mohsen Tehranizadeh[1]**

Received: 24 June 2020 / Accepted: 5 January 2022 / Published online: 15 February 2022


**Abstract**
There are not enough as recorded aftershock time histories. Therefore, intensity measures (IMs) can be used to reduce the number of necessary records. Previous studies have not dealt with the determination of a suitable IM by considering aftershock impacts. $S_a\left(T_1\right)$ has been considered as an efficient and sufficient IM in many cases. Several vector IMs of structures other than Sa(T1) were defined. The $S_a\left(T_1\right)$ of the mainshock was denoted as IM1 (the first component) in all proposed IMs. IM2s were selected such that they could be derived from the response spectrum. Therefore, the main purpose of this study is to introduce and assess several IMs considering near-field aftershock influences. For the purpose of the research, three RC frames (a one-story frame, a three-story frame, and a five-story frame) were considered. The buildings were assumed to be built in 1980s. The 2-D model of each structure was built in Opensees. Fifty-six near-field records from FEMA P-695 were selected as mainshock and aftershock records. The frames were analyzed under repeated mainshock and aftershock effects until they collapsed. Finally, the best IM was proposed. The results are valid for assessing collapse damage states, but the present study does not include other damage levels. The present investigation showed that the ratio of summation of the first mode spectral acceleration value of aftershocks on summation of the area of aftershock $S_a(T_1)$ plot as the second part of vector IM can lead to efficiency and sufficiency of the IM.

**Keywords** Vector intensity measure · Aftershock · Near-field · Low-rise frame · Collapse

## 1 Introduction

The Pacific Earthquake Engineering Research Center (PEER 2021) has developed a methodology for assessing structures. The process has been broken down into several elements (Moehile and Deierlein 2004**).** The mean annual frequency of collapse which shows the probability of collapse considering different levels of IMs for a specific IM is calculated by integrating collapse fragility curve with the hazard curve (Cornell et al. 2002; Krawinkler, et al. 2006):

$$\lambda_c = \int_{IM} P(C|im)\,|d\lambda_{IM}(im)| \tag{1}$$

In which $P(C|im)$ and $d\lambda_{IM}(im)$ are the probability of collapse given im and the probability of exceedance of IM from a specific level, respectively. An IM is an intermediate variable between ground motion hazard and the response of a structure. Efficiency and sufficiency are two factors that practitioners use to evaluate what IM is suitable for use in performance assessments (Baker and Cornell 2008).

Efficiency denotes a dispersion of the demand of a structure, while sufficiency signifies the dependency of structural responses to earthquake properties (Baker and Cornell 2008). Hazard curves for peak ground acceleration (PGA) and spectral acceleration at the fundamental period of the structure, $S_a(T_1)$, are easily accessible. Therefore, they are commonly used to assess the performance of structures.

IMs are categorized as either scalar or vector IMs. Over the past decade, a large volume of published studies has

✉ Fatemeh Soleiman Meigooni
fa.soleiman@yahoo.com

Mohsen Tehranizadeh
dtehz@yahoo.com

[1] Department of Civil and Environmental Engineering, Amirk-Abir University of Technology, 1591634311 Tehran, Iran

introduced new IMs (e.g., Yakut and Yılmaz 2008; Jayaram et al. 2010; Zhou et al. 2017; Suzuki and Iervolino 2019). Factors thought to influence IMs have been explored in several studies. For instance, many published papers describe the role of near-field impacts on structural behavior and IM determination. For example, inelastic spectral displacement has been considered as an IM in some research works (Luco and Cornell 2007; Tothong and Luco 2007). This IM can be combined with other parameters to incorporate period elongation and high mode effects. An IM has also been proposed by the second author of the paper for applying near-field shocks (Yahyaabadi and Tehranizadeh 2012).

Most studies in the field of IM have focused only on mainshocks. Preliminary work on the effects of aftershocks on the seismic demand of structures was undertaken by (Yeo and Cornell 2005). In the same vein, many studies have proposed methods for examining aftershock effects in the seismic evaluation of buildings and have considered repeated mainshock time histories as aftershocks (e.g., Bazzurro et al. 2004; Hatzigeorgiou and Beskos 2009; Luco et al. 2011; Nazari Khanmiri 2015). While a great number of investigations have also been done on the seismic evaluation of structures considering aftershocks (e.g., Iervolino et al. 2014; Jeon et al. 2015; Raghunandan et al. 2015), none have suggested building regulations that can be used for the long-term assessment of structures.

Some researchers have done by Jalayer in this field (e.g., Jalayer, et al. 2010; Ebrahimian, et al. 2014; Jalayer and Ebrahimian 2016). They proposed the most applicable method for considering aftershock effects on the seismic response and behavior of buildings. They also investigated the importance of aftershock input and concluded that aftershock sequences significantly affect structural responses (Jalayer et al. 2015). However, their studies have been concentrated mostly on the short-term effects of aftershocks. Other researchers have examined the relationship between repeating real shocks as aftershocks and the responses of buildings. Garcia, for example, claimed that the responses of structures under artificial sequences are very different from their responses under real sequences (García and Manriquez 2011; Ruiz-Garcia 2012). Goda has published several papers in which he has investigated the effects of real aftershocks on the response of structures (e.g., Goda et al. 2015). In another study, the average horizontal components of PGA, peak ground velocity (PGV), and 5% damped pseudo spectral acceleration (PSA) at different spectral periods of aftershock earthquakes were estimated for tectonically active crustal regions as a function of the aftershock-to-mainshock magnitude ratio, distance ratio, and time-averaged shear-wave velocity in the upper 30 m of soil deposits (VS30) (Kim and Shin 2017).

To determine the effects of aftershocks, Elenas et al. investigated the interrelation between seismic intensity parameters and the post-seismic damage state of structures. Several peak, energy, and spectral intensity parameters were implemented. Analytical examinations showed that both the energy and the spectral seismic intensity parameters have a strong correlation with the overall structural damage indices (Elenas et al. 2017). In 2018, Muderrisoglu et al. proposed a conditional aftershock hazard assessment method by considering the microseismic indicators of mainshocks observed at the site (Muderrioglu and Yazgan 2018). A novel formulation for the joint probability of the mainshock and aftershock spectral accelerations was proposed (Hu et al. 2019). The model can be used for mainshock-aftershock sequences. In 2019, Salami et al. investigated the influences of different types of mainshock-aftershock sequences on the seismic fragility of low-rise RC frames. They selected $S_a\left(T_1\right)$ as the IM, and ground motion data from other seismic regions were utilized. It was found that, for crustal ground motions, considering aftershocks increased the probability of the exceedance of damage to extensive and complete damage. Meanwhile, for slab and interface records, the structure experienced less damage. If the damage of the mainshock was slight or moderate, the structure was not affected by major aftershocks (Salami et al. 2019).

A review of previous proposed intensity measures, methods of aftershock collapse assessment, and some researches about near field earthquake parameters have been discussed. The study needs to consider all previously discussed parameters. This study aims to investigate the efficiency and sufficiency of vector IMs for predicting the collapse capacity of structures under near-field aftershock sequences. As $S_a(T_1)$ is not sufficient with respect to distance, 14 vector IMs were selected, among which IM1 is considered $S_a(T_1)$ of the mainshock, and IM2 is a combination of aftershock spectral properties. Three RC moment frames based on designs from the 1980s have been used, and 56 near-field records from FEMA P-695 have been used as mainshocks and aftershocks.

## 2 Considered Intensity Measures

First, the efficiency and sufficiency of $S_a(T_1)$ were eval uated. In the following sections, it is shown that the efficiency of vector-valued IM determined by degree of scatter about regression in Eq. 2. According to Table 1, $S_a(T_1)$ is

**Table 1** Standard deviation of Sa(T1) main shock

| No. Stories | 1 | 3 | 5 |
|---|---|---|---|
| Standard deviation | 0.226 | 0.161 | 0.151 |

**Table 2** *P*-values obtained from investigating the sufficiency of $S_a(T_1)$ with respect to magnitude, Distance assuming F-test for the slope of the linear regression of $S_a(T_1)$ and M and LnR. source-to-site

| No. Stories | $M$(Mainshock) | $R$(Mainshock) | $M_{\text{Avrage}}$(Aftershock) | $R_{\text{Avrage}}$(Aftershock) |
|---|---|---|---|---|
| 1 | 0 | 0 | 0.16 | 0 |
| 3 | 0.018 | 0 | 0.079 | 0 |
| 5 | 0.006 | 0.003 | 0 | 0.003 |

an efficient IM, as it has a small standard deviation. Table 1 illustrates the amount of standard deviation of one, three, and five story frames. This result corroborates that observed in Jalayer's paper (Jalayer, et al. 2010).

In order to evaluate sufficiency of $S_a(T_1)$ with respect to magnitude (M) and distance (D), it is necessary to use a unique M and D. As each aftershock sequence is made up of several earthquake records, there is not a unique M and D for each chain of earthquake records. So as to use one parameter for M and D, the average of M and D of aftershocks in each sequence were considered. If an IM is sufficient with respect to the magnitude or distance of each aftershock, it would be sufficient respect to summation of M or D. There for, the amount of average of M and D were considered for evaluation of sufficiency. Table 2 shows that $S_a(T_1)$ is not sufficient with respect to magnitude and distance. Therefore, time history properties should be considered during record selection and seismic assessment.

**Table 3** Defined vectored IMs

| No | IM2 | No | IM2 |
|---|---|---|---|
| 1 | $\sum_{i=1}^{n} \text{PGA}_i \times S_a(T_1)_{\text{Structure}}$ | 8 | $\sum_{i=1}^{n} \left(\int S_v(t)^2.dt\right)_i \times S_a(T_1)_{\text{Structure}}$ |
| 2 | $\sum_{i=1}^{n} S_a(T_1)_i \times S_a(T_1)_{\text{Structure}}$ | 9 | $\sum_{i=1}^{n} \left(\int S_a(t).S_v(t).dt\right)_i \times S_a(T_1)_{\text{Structure}}$ |
| 3 | $\sum_{i=1}^{n} S_v(T_1)_i \times S_a(T_1)_{\text{Structure}}$ | 10 | $\sum_{i=1}^{n} \left(\int \frac{S_a(t)}{t}.dt\right)_i \times S_a(T_1)_{\text{Structure}}$ |
| 4 | $\sum_{i=1}^{n} S_a(T_1)_i.S_v(T_1)_i \times S_a(T_1)_{\text{Structure}}$ | 11 | $\frac{\sum_{i=1}^{n} S_a(T_1)_i}{\sum_{i=1}^{n} \left(\int S_a(t).dt\right)_i}$ |
| 5 | $\sum_{i=1}^{n} \left(\int S_a(t).dt\right)_i \times S_a(T_1)_{\text{Structure}}$ | 12 | $\frac{\sum_{i=1}^{n} S_a(T_1)_i}{\sum_{i=1}^{n} \left(\int S_v(t).dt\right)_i}$ |
| 6 | $\sum_{i=1}^{n} \left(\int S_a(t)^2.dt\right)_i \times S_a(T_1)_{\text{Structure}}$ | 13 | $\frac{\sum_{i=1}^{n} S_a(T_1)_i}{\sum_{i=1}^{n} PGA_i}$ |
| 7 | $\sum_{i=1}^{n} \left(\int S_v(t).dt\right)_i \times S_a(T_1)_{\text{Structure}}$ | 14 | $\frac{\left(\sum_{i=1}^{n} S_a(T_1)_i\right)^2}{\sum_{i=1}^{n} \left(\int S_a(t).dt\right)_i}$ |

**Table 4** Definition of second part of IMs

| No | IM2 | Definition |
|---|---|---|
| 1 | $\sum_{i=1}^{n} \text{PGA}_i$ | Summation of PGA of all aftershock records in each chain of main shock-aftershock |
| 2 | $\sum_{i=1}^{n} S_a(T_1)_i$ | Summation of Sa(T1) of all aftershock records in each chain of main shock-aftershock |
| 3 | $\sum_{i=1}^{n} S_v(T_1)_i$ | Summation of Sv(T1) of all aftershock records in each chain of main shock-aftershock |
| 5 | $\sum_{i=1}^{n} \left(\int S_a(t)dt\right)_i$ | Summation of integral of Sa spectrum of all records in in each chain of main shock-aftershock |
| 7 | $\sum_{i=1}^{n} \left(\int S_v(t)dt\right)_i$ | Summation of integral of Sv spectrum of all records in in each chain of main shock-aftershock |

Several vector IMs of structures other than Sa(T1) were defined such that aftershocks' influences can be considered. The $S_a(T_1)$ of the mainshock was denoted as IM1 (the first component) in all proposed IMs. The aftershock response spectrum can be determined through aftershock probabilistic seismic hazard analysis (APSHA) according to Yeo and Cornell (Yeo and Cornell 2005). Some possible IM2s were investigated by the author of the paper. The IM2s were selected such that they could be derived from the response spectrum. IM2 values are given in Table 3. Table 4 provides the definitions of second components (1, 2, 3, 5, and 7). Other IM2s are produced by combining the aforementioned components, either with one another or with the $S_a(T_1)$ of the structure of mainshock records. Sv(Ti) is a spectrum defined in this article by the authors of this paper and is derived by multiplying the $S_a(T_1)$ of aftershock by $T_i$.

## 3 The Structures, Ground Motions and Analysis

In order to consider the effect of height on the results of this study, the case study buildings are selected three four-bay 2- dimensional RC frames consisting of a one-story, three-story, and five-story structure. Table 5 shows the periods of the three frames. The structures are considered to be constructed based on building code in 1980s in California. The structures are designed by author of the paper. The nonlinear behavior of RC beams and columns was modeled by utilizing the concentrated plasticity element in OpenSees. Table 5 illustrates the strength of the concrete and steel used. The dimensions of the beams and columns are shown in Tables 6 and 7, respectively.

Some researchers have concentrated on determining aftershock records (e.g., (Goda, et. al 2015)) In some research works, aftershock records are considered similar to the mainshock records, while in others, aftershocks are considered a factor of the mainshock (Lee and Foutch 2004). Li and Ellingwood utilized the Gutenberg-Richter relationship, together with the magnitude density function. They determined a factor that can be multiplied by the mainshock time history to produce the strongest aftershock (Li and Ellingwood 2007). In 2009, Hatzigeorgiou and Beskos utilized attenuation relationships to specify the PGA of aftershocks (Hatzigeorgiou and Beskos 2009). Then, they changed the records to obtain specified PGA values. Goda et al. investigated the effects of earthquake types, magnitudes, and hysteretic behavior on the peak and residual ductility demands of an inelastic single-degree-of-freedom system. An extensive dataset of real mainshock-aftershock sequences for Japanese earthquakes was developed. The records were categorized into mainshocks and aftershocks according to the time-space window (Goda et al. 2015).

**Table 5** Concrete and Steel strength (Mpa)

| Building | Concrete (Mpa) | Steel (Mpa) |
|---|---|---|
| 1Story | 17 | 455 |
| 3, and 5 Story | 24 | |

**Table 6** Dimension and reinforcement of beams

| Building | Story number (mm) | Dimension | Top | Bot | Shear |
|---|---|---|---|---|---|
| 1 Story | 1 | 300*250 | 3Φ16 | 3 Φ 16 | Φ8 @ 150 |
| 3 Story | 1, 2, and 3 | 300*300 | | | |
| 5 Story | 1, 2, and 3 | 350*350 | | | |
| | 4, and 5 | 300*250 | | | |

In this study, 56 earthquake ground motions from FEMA P-695 were used as mainshocks and aftershocks. The properties of earthquake records are illustrated in Table 8 and this table exists in FEMA P-695. For each structure, some mainshock records may lead to a collapse or instability. Moreover, it is not logical to consider the aftershock effects for records, which cause a great maximum inter-story drift ratio. According to ASCE 07-13, the maximum inter-story drift ratios for life safety and collapse prevention are 0.01 and 0.02, respectively. In this study, 0.015 was considered the limit for record purification. As such, records that cause responses greater than 0.015 were omitted. Furthermore, dynamic instability is also used for determining the collapse capacity of the structures. Dynamic instability shows that the structure will collapse under the main shock and aftershock analysis is meaningless (Figs. 1, 2).

The results for one, and three-story frames are illustrated in Fig. 3. Earthquake records are categorized in two groups including pulse like and non-pulse like. The earthquakes with inter-story drift ration greater than 0.015 or earthquakes which lead to dynamic instability were omitted. The remain records were utilized for aftershock analysis. Each of the

**Table 7** Dimension and reinforcement of columns

| Building | Story number | Dimension | Longitudinal | Shear |
|---|---|---|---|---|
| 1 Story | 1 | 300*300 | 8Φ16 | Φ8 @ 250 |
| 3 Story | 1,and 2 | 350*350 | 12Φ20 | |
| | 3 | | 8Φ16 | |
| 5 Story | 1, and 2 | 400*400 | 12Φ20 | |
| | 3, 4, and 5 | 350*350 | 8Φ16 | |

**Table 8** Properties of Earthquake records (FEMA P-695)

| ID No | Name | M | Year | NEHRP Class | V30 | Fault Type | Epicentral | Campbell | Joyner-Boore |
|---|---|---|---|---|---|---|---|---|---|
| | Pulse Record | | | | | | | | |
| 1 | Imperial Valley-06 | 6.5 | 1979 | D | 203 | Strike-slip | 27.5 | 3.5 | 0 |
| 2 | Imperial Valley-06 | 6.5 | 1979 | D | 211 | Strike-slip | 27.5 | 3.6 | 0.6 |
| 3 | Irpinia, Italy-01 | 6.5 | 1980 | B | 1000 | Normal | 30.4 | 10.8 | 6.8 |
| 4 | Superstition Hills-02 | 6.5 | 1987 | D | 349 | Strike-slip | 16 | 3.5 | 1 |
| 5 | Loma Prieta | 6.9 | 1989 | C | 371 | Strike-slip | 27.2 | 8.5 | 7.6 |
| 6 | Erzican, Turkey | 6.7 | 1992 | D | 275 | Strike-slip | 9 | 4.4 | 0 |
| 7 | Cape Mendocino | 7 | 1992 | C | 713 | Trust | 4.5 | 8.2 | 0 |
| 8 | Landers | 7.3 | 1992 | C | 685 | Strike-slip | 44 | 3.7 | 2.2 |
| 9 | Northridge-01 | 6.7 | 1994 | D | 282 | Trust | 10.9 | 6.5 | 0 |
| 10 | Northridge-01 | 6.7 | 1994 | C | 441 | Trust | 16.8 | 5.3 | 1.7 |
| 11 | Kocaeli, Turkey | 7.5 | 1999 | B | 811 | Strike-slip | 5.3 | 7.4 | 3.6 |
| 12 | Chi-Chi, Taiwan | 7.6 | 1999 | D | 306 | Trust | 26.7 | 6.7 | 0.6 |
| 13 | Chi-Chi, Taiwan | 7.6 | 1999 | C | 714 | Trust | 45.6 | 7.7 | 1.5 |
| 14 | Duzce, Turkey | 7.1 | 1999 | D | 276 | Strike-slip | 1.6 | 6.6 | 0 |
| | No Pulse Record | | | | | | | | |
| 15 | Gazli, USSR | 6.8 | 1979 | C | 660 | Trust | 12.8 | 5.5 | 3.9 |
| 16 | Imperial Valley-06 | 6.5 | 1979 | D | 223 | Strike-slip | 6.2 | 4 | 0.5 |
| 17 | Imperial Valley-06 | 6.5 | 1979 | D | 275 | Strike-slip | 18.9 | 8.4 | 7.3 |
| 18 | Nahanni, Canada | 6.8 | 1985 | C | 660 | Trust | 6.8 | 9.6 | 2.5 |
| 19 | Nahanni, Canada | 6.8 | 1985 | C | 660 | Trust | 6.5 | 4.9 | 0 |
| 20 | Loma Prieta | 6.9 | 1989 | C | 376 | Strike-slip | 9 | 10.7 | 3.9 |
| 21 | Loma Prieta | 6.9 | 1989 | C | 462 | Strike-slip | 7.2 | 3.9 | 0.2 |
| 22 | Cape Mendocino | 7 | 1992 | C | 514 | Trust | 10.4 | 7 | 0 |
| 23 | Northridge-01 | 6.7 | 1994 | C | 380 | Trust | 8.5 | 8.4 | 0 |
| 24 | Northridge-01 | 6.7 | 1994 | D | 281 | Trust | 3.4 | 12.1 | 0 |
| 25 | Kocaeli, Turkey | 7.5 | 1999 | D | 297 | Strike-slip | 19.3 | 5.3 | 1.4 |
| 26 | Chi-Chi, Taiwan | 7.6 | 1999 | C | 434 | Trust | 28.7 | 6.5 | 0.6 |
| 27 | Chi-Chi, Taiwan | 7.6 | 1999 | C | 553 | Trust | 8.9 | 11.2 | 0 |
| 28 | Denali, Alaska | 7.9 | 2002 | C | 553 | Strike-slip | 7 | 8.9 | 0 |

frame under a specific main shock will collapse with different numbers of sequential aftershocks. Fig. 2 illustrates the number of aftershock records that leads to collapse of each frame. It shows that for the one-story frame, the number of aftershocks for collapse of structure is approximately less than 10 records. This number is five for three and five story frames. According to Fig. 2. The shorter a building, the greater number of aftershock records need to collapse.

## 4 Efficiency of IMs for Collapse Capacity Prediction

The efficiency of a scalar IM indicates a lower dispersion among the capacity values. For a vector IM, efficiency is defined as the degree of scattering of capacity concerning the regression in Eq. 2. The scattering in Eq. 2 can be determined through Eq. 3. Therefore, a vector IM is more efficient if it has a lower standard deviation according to Eq. 3. From another viewpoint, efficiency illustrates whether there is a high correlation between $IM_1$ and $IM_2$. Equation 4 can be utilized to determine the correlation coefficient in which $cov()$ represents the convenience between variables, and $\sigma_{lnIM_1}$ and $\sigma_{lnIM_2}$ are the standard deviation of $lnIM_1$ and $lnIM_2$, respectively. The correlation between $lnIM_1$ and $lnIM_2$ is shown for some $IM_2$ s for a one-story building in Fig. 4. The period of frames are available in Table 9.

The correlation coefficient and standard deviation are available for three frames in Tables 10, 11, and 12. The maximum values of the correlation coefficient for the one-, three-, and five-story buildings were obtained from $IM_2(11)$, $IM_2(12)$, and $IM_2(12)$, respectively. Figure 4 shows the correlation between ln Sa and IM2 considering the IM2(11) and IM2(12) parameters for the one-story structure.

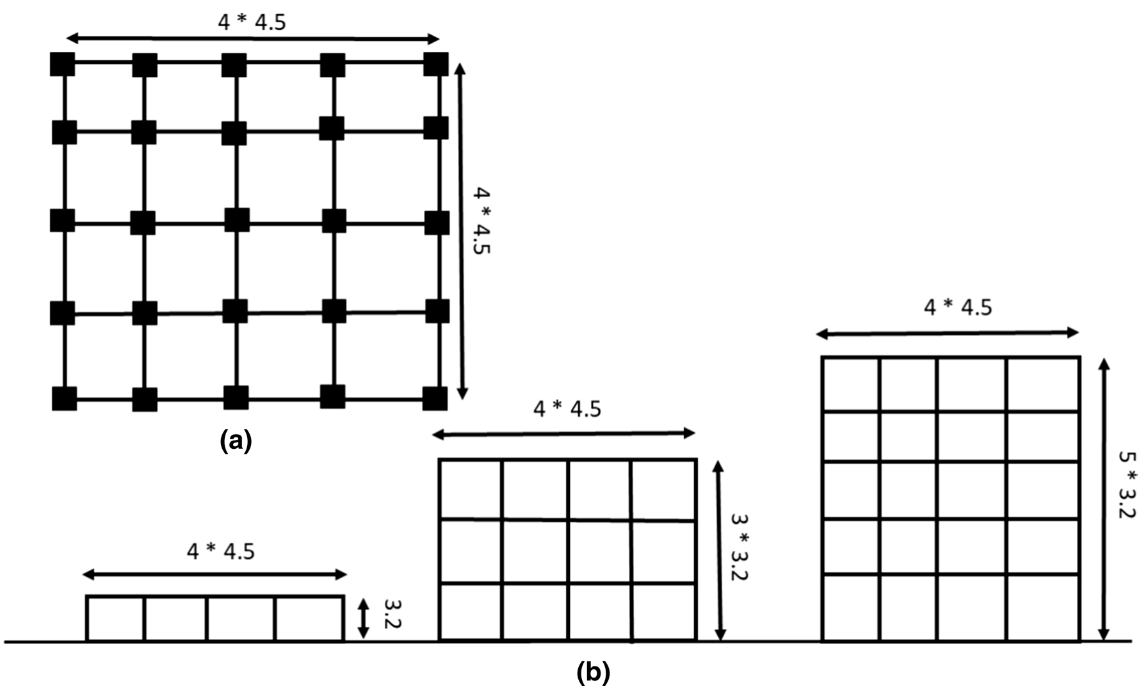


**Fig. 1** **a** Plan and, **b** Elevation of considered buildings

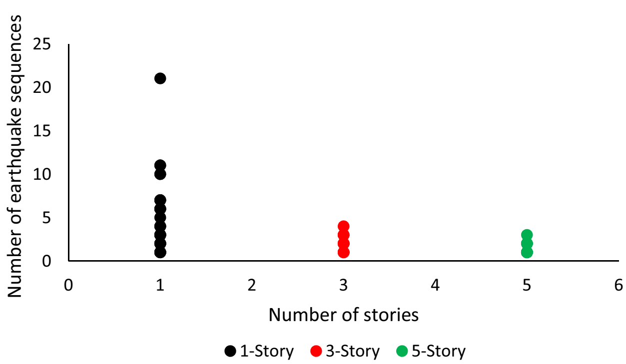


**Fig. 2** The number of aftershocks needed for collapse of the frames

Using an efficient vector IM leads to a reduction in the number of earthquakes required for the estimation of a structural response. Equation 5 can be used to calculate the standard error of capacity associated with a sample size of $n_s$. Table 10 shows the standard error of all $\text{IM}_2$ s for each building as percentages.

$$\mu_{\ln IM_1|IM_2=im_2} = \alpha_0 + \alpha_1 \ln IM_2 \tag{2}$$

$$\sigma_{\ln IM_1|IM_2} = \left[ \sum_{i=1}^{n} \left( \ln IM_{1i} - \ln \overline{IM_{1i}} \right)^2 / (n-2) \right]^{\frac{1}{2}} \tag{3}$$

$$\rho = \frac{\text{cov}(\ln IM_1, \ln IM_2)}{\sigma_{\ln IM_1} \sigma_{\ln IM_2}} \tag{4}$$

$$SE = \frac{\sigma_{\ln IM_1|IM_2}}{\sqrt{n_s}} \tag{5}$$

## 5 Sufficiency of IMs for Collapse Capacity Prediction Considering the Magnitude and Source to Site Distance

A sufficient IM has an independent distribution of the ground motion properties (e.g., magnitude and distance). In scalar IMs, sufficiency, with respect to M and R, is determined through a linear regression between the properties and observed capacity through Eq. 6, in which coefficients $\beta_0$ and $\beta_1$ can be determined from the linear regression, and x can be M or $LnR$. The student-t distribution can be assumed for $\beta_1$, and an F-test can be utilized to determine the significance of $\beta_1$. A p-value of less than 0.05 shows insufficiency. It can be seen that $IM_1$ is insufficient with respect to M and lnR. To determine the sufficiency of Vectored-M, the residual capacity of Eq. 1 for $Ln_R$ or M is used in Eq. 6 instead of collapse capacity Tables 13 and 14.

$$\mu_{\ln IM_1} = \beta_0 + \beta_1 x \tag{6}$$

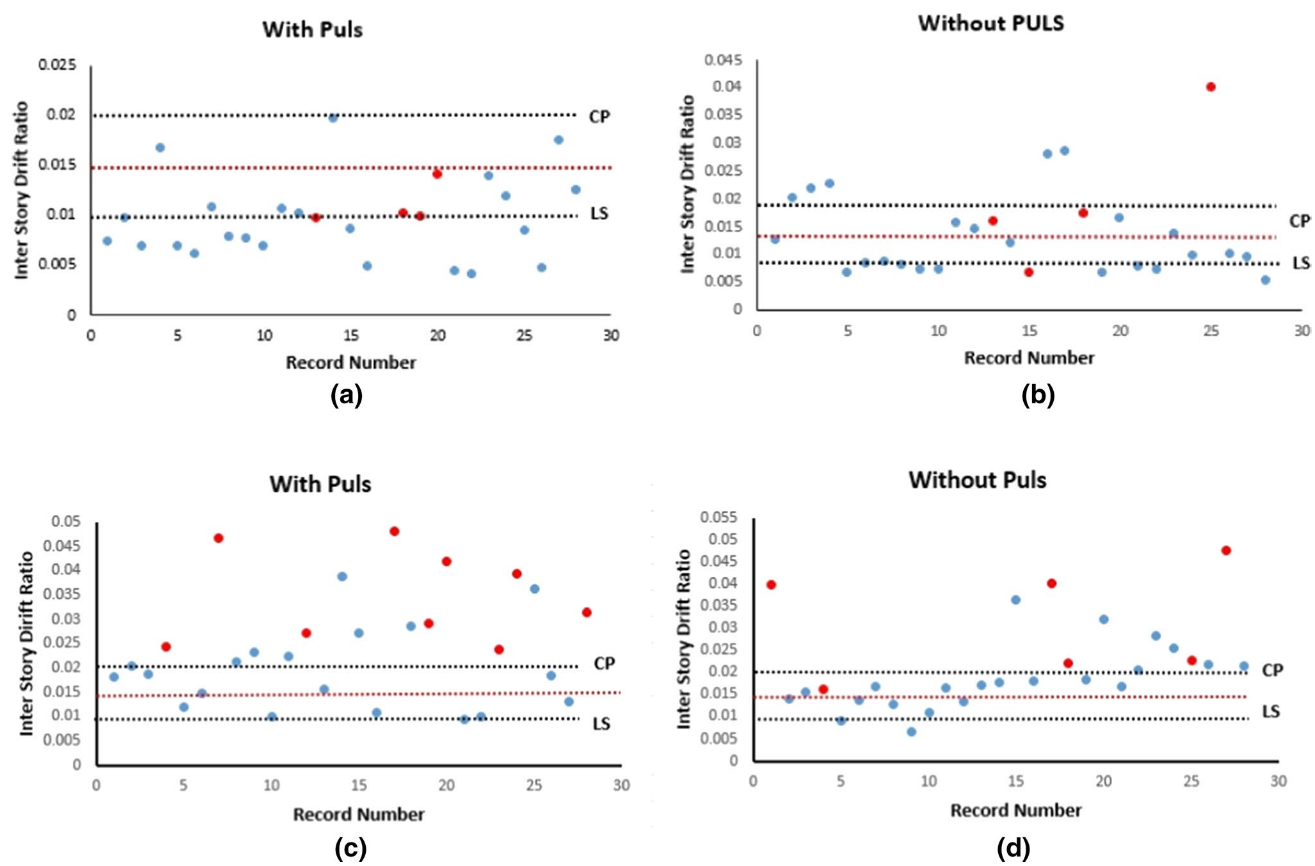


**Fig. 3** Purification of earthquake records

Other research studies have used this method to determine sufficiency (Luco and Cornell 2007), (Baker and Cornell 2008), (Tothong and Cornell 2008), and (Bradley, et al. 2009). Figure 6 illustrates the results. Regarding the relationship between $IM_1$ as a scalar IM with respect to M and *LnR* for a one-story building. It can be concluded that IM1 is insufficient with respect to M and *LnR*, as the p-values from the F-test are less than 0.05. Therefore, it is necessary to consider the magnitude and distance of the earthquake record. A unique magnitude and distance cannot be dedicated to a chain of sequences from an earthquake, as it is made up of several time histories. Distance and magnitude were considered as the average of all earthquakes in each series. The p-values for M and R for all vector IMs are available in Tables 15 and 16, respectively. Figures 5 and 6 illustrate the results for the one-story frame. $IM_2(11)$ shows the best sufficiency of all IM2s.

In order to calculate collapse probability, 46 main shock records were considered where each main shock was followed by 50 chains of aftershock (Fig. 7). The Fig. 7 illustrates the procedure which was proposed in this study. Thus, in this study n and m are 28 and 50 respectively. Variable n shows the number of earthquakes that were used as the main shocks and variable m denotes to the number of chains that follow each mainshock. In total there is (28*150) 1400 main shock- aftershock sequences. Collapse probability for a vector IM can be calculated via logistic regression according to the Eq. 7. Note that the return period is considered to be equal to a specific measure and all the main shock records are scaled to have $IM_1 = S_a(T_1)$ mainshock, after which unscaled records were imposed to the frames as aftershock. In order to calculate collapse probability, $\mathrm{im}_1$, $\mathrm{im}_2$, $a$, and $b$ should be determined.$\mathrm{im}_1$ is $S_a(T_1)$ of main shock. This parameter depends on the considered return period and is extract from main shock spectrum of the region. All main shocks are scaled to have $\mathrm{IM}_1 = \mathrm{im}_1$. Unscaled main shocks are utilized as aftershock and imposed to the structure until the collapse happens. There for there are 1400 amin shock-aftershock sequences. The parameter ($IM_2(11)$) which is the ratio of summation of the first mode spectral acceleration value of aftershocks on summation of the area of aftershocks $S_a(T_1)$ plot of each chain is calculated. According to the results of logistic regression the mount of a, and b are extract. In order to obtain $im_2$, the amount Eq. 8 should be determined.

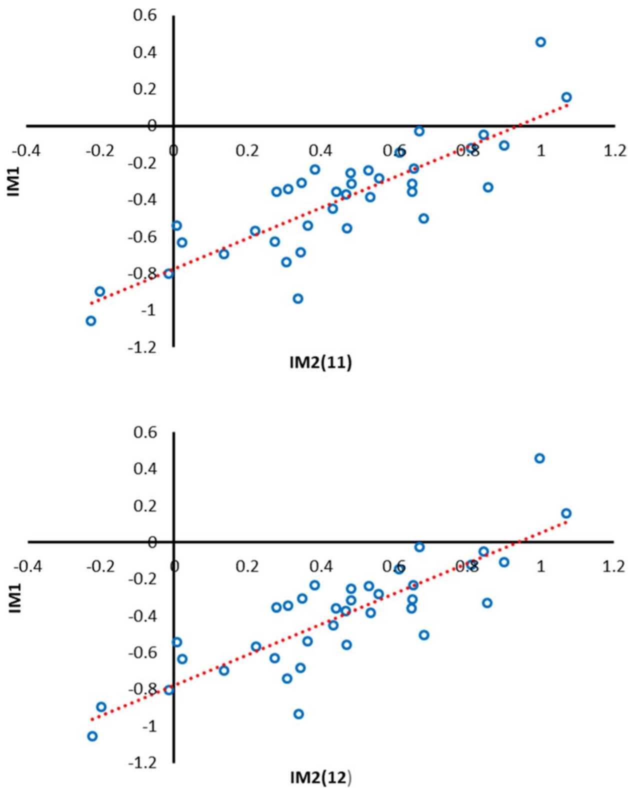


**Fig. 4** Correlation between the collapse capacity of the 1-story structure and different IM2(11) and IM2(12)

**Table 9** Period of the structures

| Number of stories | Fundamental period (s) |
|---|---|
| 1 | 0.454 |
| 3 | 0.93 |
| 5 | 1.238 |

$$P(Collapse|IM_1 = im_1, IM_2 = im_2) = {}^{1}\!/_{1 + e^{-(a+b\,mi_2)}} \quad (7)$$

$$\sum_{i=1}^{i=na} S_a(T_1) \Big/ \sum_{i=1}^{i=na} \int S_a(T_1) \quad (8)$$

In which na is the number of aftershocks that follow each mainshock. The expected number of aftershocks with a specific magnitude can be determined through Epidemic-Type Aftershock Sequence (ETAS) ($N_{ETAS}$)(Tavakolietal.2018). Therefore, na is equal to the $N_{ETAS}$ for each earthquake magnitude, as Eq. 8 is a fraction, the amount of $N_{ETAS}$ in the face and dominator are omitted. Therefore, $im_2$ can be derived by Eq, 9.

$$im_2 = S_a(T_1) \Big/ \int S_a(T_1) \quad (9)$$

The amount of $S_a(T_1)$ of aftershock can be determined by Aftershock spectrum for a specific return period. $\int S_a(T_1)$ is the area under the aftershock spectrum which obtained by aftershock probabilistic hazard analysis. Knowing $im_2$, collapse probability can be calculated through Eq. 7. In order to illustrate the procedure, the collapse probability of 1,3 and 5 story frames in Sect. 3 are determined. The results are as bellow. It should be mentioned that the return period is considered to be 10% in 50 years. Table 13 and 14 show the results.

It can be concluded the number of stories doesn't have consider effect on probability of collapse.

## 6 Results

An overview of the results is provided in Table 18. The correlation coefficient has been categorized into four groups according to (Rumsey 2016) (Table 17). According to the

**Table 10** Correlation, P-value, and standard deviation of 1-story frame

| Parameter | 1 | 2 | 3 | 4 | 5 | 6 | 7 | 8 | 9 | 10 | 11 | 12 | 13 | 14 |
|---|---|---|---|---|---|---|---|---|---|---|---|---|---|---|
| Correlation | 0.452 | 0.453 | 0.453 | 0.4431 | 0.455 | 0.447 | 0.526 | 0.568 | 0.572 | 0.451 | 0.839 | 0.671 | 0.604 | 0.437 |
| P-value | 0.017 | 1E-07 | 2E-15 | 8E-16 | 0.477 | 0.295 | 0.001 | 9E-23 | 2E-24 | 8E-11 | 2E-27 | 6E-24 | 9E-12 | 5E-16 |
| STD | 1.044 | 0.91 | 0.91 | 0.9957 | 1.006 | 1.205 | 0.812 | 0.821 | 0.869 | 1.047 | 0.302 | 0.423 | 0.396 | 0.838 |

**Table 11** Correlation, P-value, and standard deviation of 3-story frame

| Parameter | 1 | 2 | 3 | 4 | 5 | 6 | 7 | 8 | 9 | 10 | 11 | 12 | 13 | 14 |
|---|---|---|---|---|---|---|---|---|---|---|---|---|---|---|
| Correlation | 0.55 | 0.399 | 0.399 | −0.001 | 0.565 | −0.137 | 0.568 | 0.307 | −0.05 | 0.572 | 0.751 | 0.87 | 0.399 | 0.131 |
| P-value | 0.134 | 0.017 | 1E-10 | 2E-10 | 6E-04 | 0.111 | 5E-09 | 9E-14 | 2E-13 | 3E-05 | 0.002 | 2E-12 | 0.161 | 0.295 |
| STD | 0.828 | 0.553 | 0.553 | 0.6396 | 0.647 | 0.792 | 0.561 | 0.583 | 0.632 | 0.702 | 0.34 | 0.347 | 0.414 | 0.58 |

**Table 12** Correlation, P-value, and standard deviation of 5-story frame

| Parameter | 1 | 2 | 3 | 4 | 5 | 6 | 7 |
|---|---|---|---|---|---|---|---|
| Correlation | 0.583 | 0.626 | 0.626 | 0.2888 | 0.633 | 0.502 | 0.[illegible] |
| P-value | 0.005 | 1E-07 | 3E-15 | 7E-14 | 4E-06 | 5E-04 | 8E[illegible] |
| STD | 0.923 | 0.449 | 0.449 | 0.6344 | 1.119 | 1.119 | 0.[illegible] |

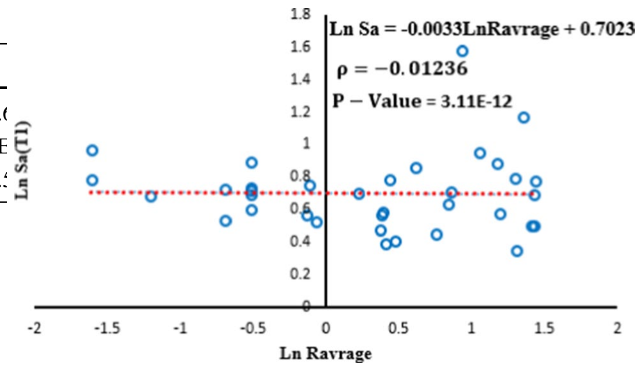


**Fig. 5** Testing the sufficiency of Sa(T1) with respect to M and R for collapse capacity prediction of the 1-story structure: M

**Table 13** $im_1.b.a$ of frames

| Number of Stories | $im_1$ | $a$ | $b$ |
|---|---|---|---|
| 1 | 0.8425 | 1.4089 | − 2.3462 |
| 3 | 0.5012 | 2.0897 | − 4.7194 |
| 5 | 0.4539 | 2.0833 | − 11.1019 |

**Table 14** $im_2$, $a$, and $b$ of frames

| Number of stories | $S_a(T_1)$ | $\int S_a(T_1)$ | $im_2$ | P(collapse) (%) |
|---|---|---|---|---|
| 1 | 1.036 | 2.6697 | 0.3879 | 62.2 |
| 3 | 0.896 | 2.6697 | 0.3357 | 62.3 |
| 5 | 0.7262 | 2.6697 | 0.272 | 71.8 |

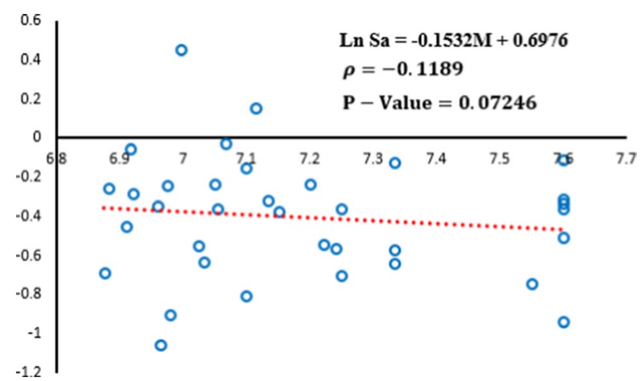


**Fig. 6** Testing the sufficiency of Sa(T1) with respect to M and R for collapse capacity prediction of the 1-story structure: LnR

previous sections, an efficient IM assumes that a t-test will yield a p-value of less than 0.05, while a sufficient IM (using the F-test) should yield a p-value of above 0.05. Considering this, an acceptable and unacceptable p-value has been shown with A and No, respectively. According to the data in Table 18, IM2(11) and IM2(12) have the best correlation

**Table 15** P-value of IM2 respect to M

| St No | 1 IM2 | 2 | 3 | 4 | 5 | 6 | 7 | 8 | 9 | 10 | 11 | 12 | 13 | 14 |
|---|---|---|---|---|---|---|---|---|---|---|---|---|---|---|
| 1 | 0.207 | 0.296 | 0.275 | 0.128 | 0.102 | 0.012 | 0.344 | 0.075 | 3E-09 | 2E-07 | 0.0541 | 4E-05 | 0.01 | 2E-10 |
| 3 | 2E-05 | 0.002 | 0.002 | 3E-04 | 3E-04 | 3E-05 | 0.001 | 1E-03 | 0.0004 | 1E-04 | 0.0971 | 0.0851 | 0.024 | 0.001 |
| 5 | 0.015 | 2E-06 | 2E-06 | 2E-04 | 0.001 | 0.079 | 3E-05 | 5E-04 | 0.0176 | 0.003 | 2E-06 | 1E-05 | 4E-05 | 1E-06 |

**Table 16** P-Value of IM2s respect to LnR

| St No | 1 IM2 | 2 | 3 | 4 | 5 | 6 | 7 | 8 | 9 | 10 | 11 | 12 | 13 | 14 |
|---|---|---|---|---|---|---|---|---|---|---|---|---|---|---|
| 1 | 0.184 | 0.45 | 0.45 | 0.252 | 0.238 | 0.039 | 0.3 | 0.319 | 0.461 | 0.175 | 1E-08 | 2E-05 | 8E-06 | 0.365 |
| 3 | 0.063 | 0.41 | 0.41 | 0.687 | 0.347 | 0.144 | 0.495 | 0.487 | 0.411 | 0.248 | 0.1794 | 0.209 | 0.3983 | 0.271 |
| 5 | 0.041 | 0.162 | 0.162 | 0.404 | 0.181 | 0.008 | 0.451 | 0.232 | 0.028 | 0.114 | 0.1909 | 0.2831 | 0.4988 | 0.14 |

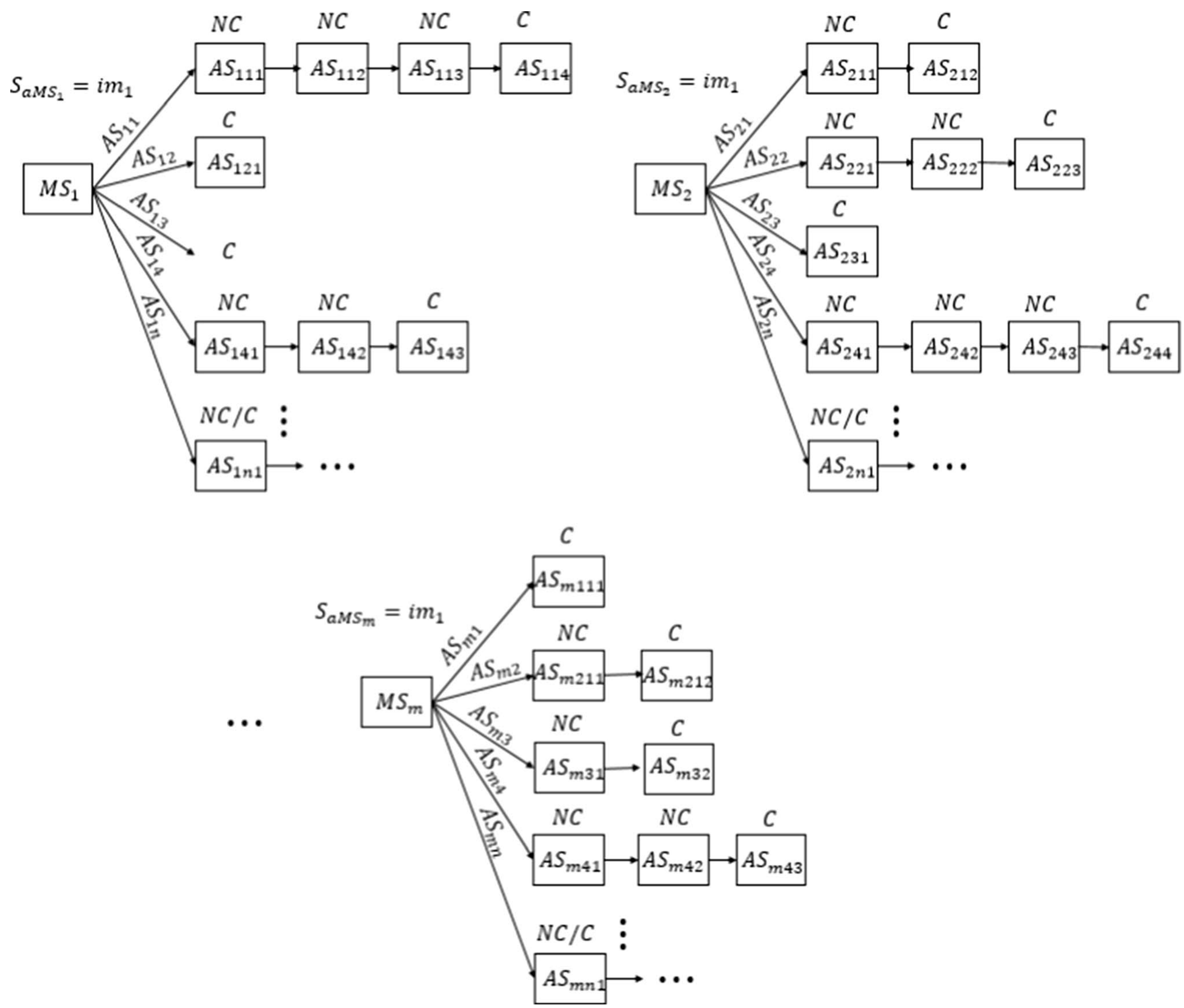


**Fig. 7** Chemotic diagram of the sequential analysis procedure

of any two IM2s. However, it seems that IM2(12) is not sufficient with respect to magnitude. IM2(14) has the lowest level of correlation with the other IM2s. Other IM2s were also found not to be sufficient with respect to M. Therefore, IM2(11) is the best candidate for the second main IM. As a result, (Sa(T1), IM (11)) is the most likely acceptable IM for the seismic evaluation of short buildings when aftershock impacts are considered.

**Table 17** Categorization of correlation coefficient

| Correlation Coef | Group | Abbreviation |
|---|---|---|
| 0.3 | Weak | W |
| 0.5 | Moderate | M |
| 0.7 | Strong | S |
| 1 | Excellent | E |

## 7 Conclusions

The aim of this study is to investigate several new vector IMs in order to compare the proposed IMs.

Three low-rise RC frames were considered and analyzed under the 56 near-field earthquake record situations taken from FEMA P-695. The results show that the $S_a(T_1)$ of the mainshock was insufficient with respect to M. Therefore, new vector records were introduced. The $S_a(T_1)$ of the mainshock was considered the first component in all the new IMs.

The present investigation showed that $(S_a(T_1).IM_2(11))$ is the most suitable case among other proposed IMs, as it is

**Table 18** Summery of the results

| | Correlation | | | Standard Deviation | | | *P*-Value IM1 & IM2 | | | *P*-Value Maverage | | | *P*-Value Ravrage | | |
|---|---|---|---|---|---|---|---|---|---|---|---|---|---|---|---|
| | 1 | 3 | 5 | 1 | 3 | 5 | 1 | 3 | 5 | 1 | 3 | 5 | 1 | 3 | 5 |
| 1 | M | S | S | 1.044 | 0.828 | 0.923 | A | NO | A | A | NO | NO | A | A | A |
| 2 | M | M | S | 0.91 | 0.553 | 0.449 | A | NO | A | A | NO | NO | A | A | A |
| 3 | M | M | S | 0.91 | 0.553 | 0.449 | A | A | A | A | NO | NO | A | A | A |
| 4 | M | W | W | 0.996 | 0.64 | 0.634 | A | A | A | A | NO | NO | A | A | A |
| 5 | M | S | S | 1.006 | 0.647 | 1.119 | NO | A | A | A | NO | NO | A | A | A |
| 6 | M | W | S | 1.205 | 0.792 | 1.119 | NO | NO | A | A | NO | A | A | A | A |
| 7 | S | S | S | 0.812 | 0.561 | 0.548 | A | A | A | A | NO | NO | A | A | A |
| 8 | S | M | S | 0.869 | 0.583 | 0.679 | A | A | A | A | NO | NO | A | A | A |
| 9 | S | W | M | 0.869 | 0.632 | 0.936 | A | A | A | NO | NO | A | A | A | A |
| 10 | M | S | S | 1.047 | 0.702 | 0.79 | A | A | A | NO | NO | NO | A | A | A |
| 11 | E | E | E | 0.302 | 0.34 | 0.455 | A | A | NO | A | A | NO | NO | A | A |
| 12 | S | E | E | 0.423 | 0.347 | 0.512 | A | A | A | NO | A | NO | NO | A | A |
| 13 | S | M | W | 0.396 | 0.414 | 0.559 | A | NO | A | A | A | NO | NO | A | A |
| 14 | M | W | W | 0.838 | 0.58 | 0.442 | A | NO | A | NO | NO | NO | A | A | A |

both efficient and sufficient $IM_2(11)$ is the ratio of summation of the first mode spectral acceleration value of aftershocks on summation of the area of aftershock spectrum $S_a(T_1)$ plots. Thus, by utilizing this IM, the number of analyses needed to estimate the structural response of a building can be decreased. Also, earthquake records can be considered independently of their magnitude and distance from the building. Furthermore, the efficiency and sufficiency of the proposed IMs can increase the reliability of seismic assessments.

The current study has examined only RC frames. The research does not consider all damage states and evaluates only the structures at a collapse damage level.

## References


Baker JW, Cornell CA (2008) Vector-valued intensity measures for pulse-like near-fault ground motions. Eng Struct 30:1048–1057

Bazzurro P, Cornell CA, Menun C, Luco N, and Motahari M (2004) Advanced seismic assessment guidelines. PEER Lifelines Program, Pacific Gas & Electric (PG&E)

Bradley BA, Cubrinovski M, Dhakal RP, MacRae GA (2009) Intensity measures for the seismic response of pile foundations. Soil Dyn Earthq Eng 29(6):1046–1058

Cornell CA, Jalayer F, Hamburger RO, Foutch DA (2002) Probabilistic basis for 2000 SAC Federal Emergency Management Agency steel moment frame guidelines. J Struct Eng 128(4):526–533

Ebrahimian H et al (2014) A performance-based framework for adaptive seismic aftershock risk assessment. Earthq Eng Struct Dyn 43(14):2179–2197

Elenas A, Siouris IM, and Plexidas A (2017) A study on the interrelation of seismic intensity parameters and damage indices o structures under mainshock-aftershock seismic sequences. 16th World Conference on Earthquake, 16WCEE. Santiago

García JR, Negrete Manriquez JC (2011) Evaluation of drift demands in existing steel frames under as-recorded far-field and near-fault mainshock–aftershock seismic sequences. Eng Struct 33(2):621–634

Goda K (2015) Record selection for aftershock incremental dynamic analysis. Earthq Eng Struct Dynam 44:1157–1162

Goda K, Wenzel F, and Risi RD (2015) Empirical assessment of non-linear seismic demand of mainshock–aftershock ground-motion sequences for Japanese earthquakes. Frontiers in Built Environment 1

Hatzigeorgiou GD, Beskos DE (2009) Inelastic displacement ratios for SDOF structures subjected to repeated earthquakes. Eng Struct 31(11):2744–2755

Hu S, Tabandeh A, and Gardoni P (2019) Modeling the joint probability distribution of main shock and aftershock spectral accelerations. 13th International Conference on Applications of Statistics and Probability in Civil Engineering, ICASP13. Seoul

Iervolino I, Giorgio M, Chioccarelli E (2014) Closed-form aftershock reliability of damage-cumulating elastic-perfectly-plastic systems. Earthq Eng Struct Dynam 43:613–625

Jalayer F, Asprone D, Prota A, Manfredi G (2010) A decision support system for post-earthquake reliability assessment of structures subjected to aftershocks: an application to L'Aquila earthquake, 2009. Bull Earthq Eng 9(4):997–1014

Jalayer F, Ebrahimia H, and Manfredi G (2015) Towards quantifying the effects of aftershocks in seismic risk assessment. 12th International Conference on Applications of Statistics and Probability in Civil Engineering, ICASP12. Vancouver

Jalaye F, and Ebrahimian H (2016) Seismic risk assessment considering cumulative damage due to aftershocks. Earthquake Engineering & Structural Dynamics

Jayaram N, Bazzurro P, Mollaioli F, De Sortis A, and Bruno S (2010) Prediction of structural response of reinforced concrete frames subjected to earthquake ground motions. 9th US National and 10th Canadian Conference on Earthquake Engineering. Toronto, 428–437

Jeon J-S, DesRoches R, Lowes LN, Brilakis I (2015) Framework of aftershock fragility assessment–case studies: older California reinforced concrete building frames. Earthq Eng Struct Dynam 44:2617–2636

Kim B, Shin M (2017) A model for estimating horizontal aftershock ground motions for active crustal regions crustal regions. Soil Dyn Earthq Eng 92:165–175

Krawinkler H, Zareian F, Medina RA, Ibarra LF (2006) Decision support for conceptual performance-based design. Earthquake Eng Struct Dynam 35:115–133

Lee K, and Foutch DA (2004) Performance evaluation of damaged steel frame buildings subjected to seismic loads. Journal of Structural Engineering 130: 588–599.

Li Q, Ellingwood BR (2007) Performance evaluation and damage assessment of steel frame buildings under main shock–aftershock earthquake sequences. Earthq Eng Struct Dynam 36:405–427

Luco N, Cornell CA (2007) Structure-specific scalar intensity measures for nearsource and ordinary earthquake ground motions. Earthq Spectra 23(2):357–392

Luco N, Gerstenberger MC, Uma SR, Ryu H, Liel AB, and Raghunandan M (2011) A methodology for post-mainshock probabilistic assessment of building collapse risk. Ninth Pacific Conference on Earthquake Engineering. Auckland

Moehile J, and Deierlein GG (2004) A framework methodology for Performance-Based Earthquake Engineering. 13th World Conference on Earthquake Engineering. Vancouver

Muderrioglu, Ziya, and Ufuk Yazgan. "Aftershock Hazard Assessment Based on Utilization of Observed Main Shock Demand." *Earthquake Spectra* 34, no. 2 (2018).

Nazari Khanmiri N (2015) Methodology and applications for integrating eartquake aftershock Risk into performance-based seismic design. PhD Thesis, Department of Civil and Environmental Engineering, Colorado State University, Colorado

PEER (2021) Paxifice Earthquake Engineering Research center. 2021. https://peer.berkeley.edu/.

Raghunandan M, Liel AB, and Luco N Aftershock collapse vulnerability assessment of reinforced concrete frame structures. Earthquake Engineering and Etructural Dynamics, 2015: 419–439

Ruiz-Garcia J (2012) Mainshock-aftershock ground motion features and their influence in building's seismic response. J Earthquake Eng 16:719–737

Rumsey DJ (2016) 2nth Edition vols

Salami MR, Kashani MM, Goda K (2019) Influence of advanced structural modeling technique, mainshock-aftershock sequences, and ground-motion types on seismic fragility of low-rise RC structures. Soil Dyn Earthq Eng 117:263–279

Suzuki A, and Iervolino I (2019) Hazard-consistent intensity measure conversion of fragility curves. 13th International Conference on Applications of Statistics and Probability in Civil Engineering, ICASP13. Seoul

Tothong, P, and CA Cornell. "Structural performance assessment under near-source pulse-like using advanced ground motion intensity measures." *Earthquake Engineering and Structural Dynamics* 37, no. 7 (2008).

Tothong P, Luco N (2007) Probabilistic seismic demand analysis using advanced ground motion intensity measures. Earthquake Eng Struct Dynam 36(13):1837–1860

Yahyaabadi A, and Tehranizadeh M (2012) Development of an improved intensity measure in order to reduce the variability in seismic demands under near-fault ground motions. Journal of Earthquake and Tsunami 6(2)

Yakut A, and Hazım Y (2008) Correlation of deformation demands with ground motion intensity. Journal of Structural Engineering 134(12)

Yeo GL, and Cornell CA (2005) Stochastic characterization and decision bases under time-dependent aftershock risk in performance-based earthquake engineering. PEER Report 2005/13, Department of civil andenvironmental engineering, Stanford University, Berkeley: Pacific Earthquake Engineering Research Center

Zhou Y, Ge P, Li M, and Han J An area-based intensity measure for incremental dynamic analysis under two-dimensional ground motion input. The Structural Design of Tall and Special Buildings 26(12)